



# Density measurement of Ti–X (X = Cu, Ni) melts and thermodynamic correlations

Manabu Watanabe<sup>1,\*</sup> , Masayoshi Adachi<sup>1</sup>, and Hiroyuki Fukuyama<sup>1,\*</sup> 

<sup>1</sup>Institute of Multidisciplinary Research for Advanced Materials, Tohoku University, Sendai 980-8577, Japan

Received: 28 August 2018

Accepted: 31 October 2018

Published online:

7 November 2018

© Springer Science+Business Media, LLC, part of Springer Nature 2018

## ABSTRACT

The densities of Ti–X (X = Cu, Ni) melts were measured by a combination of electromagnetic levitation and a static magnetic field. The static magnetic field suppressed surface oscillation of the levitated sample droplet, which enhances the accuracy and precision of density measurements. Densities of the Ti–X melts varied linearly over a wide temperature range including a supercooled temperature region. The excess volumes of Ti–X were slightly negative over the entire composition range. These results are discussed within a thermodynamic framework considering the relationship between excess volume and thermodynamic properties such as excess Gibbs energy and enthalpy of mixing. The excess volume correlated more strongly with excess Gibbs energy for various binary alloy systems than with the enthalpy of mixing.

## Introduction

Correlations between excess volume and thermodynamic functions of liquid-state binary alloys have been reported since 1937 [1, 2]. We have investigated the correlation between excess volume ( $V^E$ ) and excess Gibbs energy ( $G^E$ ) of 20 binary alloy melts (0.5 mole fraction) [3, 4]. We reported that compound-forming systems have negative  $V^E$  with negative  $G^E$  in liquid states. Conversely, alloy systems exhibiting immiscibility have positive  $V^E$  with positive  $G^E$  in liquid states. In addition, alloy systems exhibiting order–disorder transitions have positive  $V^E$  with negative  $G^E$  in liquid states.

The Ti–Cu and Ti–Ni systems are compound-forming systems [5]. On the basis of the foregoing trend, we expect that these systems have negative  $V^E$ .

In 2004, Krasovskyy and Naidich [6] used the sessile drop method to measure the densities of the Ti–Cu melts. In 2013, Amore et al. [7] used an electromagnetic levitation (EML) method to measure the densities of Ti–Cu melts. The composition dependence of density reported by Krasovskyy and Naidich [6] showed positive deviation from the ideal solution model. Conversely that reported by Amore et al. [7] showed a negative deviation.

In the case of Ti–Ni melts, Zou et al. [8] measured the densities over a limited range of compositions, namely a Ni mole fraction range of 0.45–0.55 by an electrostatic levitation (ESL) method. Thus, the  $V^E$  of Ti–Cu and Ti–Ni melt have yet to be well established.

In this study, we aimed to accurately measure the density of Ti–X (X = Cu or Ni) melts using a combination of EML and a static magnetic field [3]. A static

Address correspondence to E-mail: w-manabu@mail.tagen.tohoku.ac.jp; hiroyuki.fukuyama.b6@tohoku.ac.jp

magnetic field was applied to a levitated sample droplet to suppress the surface oscillation and translational motion of the droplet, which enables high-precision density measurements. On the basis of these results, we discuss  $V^E$  in terms of thermodynamic properties such as mixing enthalpy and  $G^E$  for various binary alloy systems.

## Experimental

Full details of the levitation method for the density measurements are given in previous paper [3]. Samples were prepared using Cu (99.99 mass% purity), Ni (99.996 mass% purity) and Ti (99.9 mass% purity), which were alloyed by arc melting. The sample was levitated electromagnetically in an Ar-5 vol% H<sub>2</sub> gas atmosphere. A static magnetic field of 2.0–4.0 T was then applied to the sample droplet by a superconducting magnet (JMTD-10T 120SSFX, Japan Superconductor Technology, Kobe, Japan) to suppress sample oscillation and translational motion. Side-view images of the sample were recorded for 10 s in each measurement at a frame rate of 200 fps, i.e., sample images were obtained from an average of 2000 images taken by a high-speed camera (MC1310, Mikrotron, Unterschleißheim, Germany). The sample radius ( $r$ ) was determined by fitting of the sample edge with a series of Legendre polynomials, and its volume ( $V$ ) was calculated assuming that the sample shape was rotationally symmetrical around the vertical axis. Stainless steel balls (diameters: 4.760, 6.366 and 6.999 mm) were used as a calibration standard to obtain the real length of the sample droplet. The sample mass ( $m$ ) was measured before and after the density measurements, and its average value was used for the density determination. The sample temperature was measured with a single-color pyrometer, which was calibrated to the liquidus temperature of each alloy [5]. Because titanium easily absorbs oxygen, oxygen dissolved in Ti before and after measurement was quantitatively analyzed by LECO analysis (TC-436, LECO, St. Joseph).

## Results

### Ti

The dissolved oxygen contents in the Ti sample measured before and after the density measurements

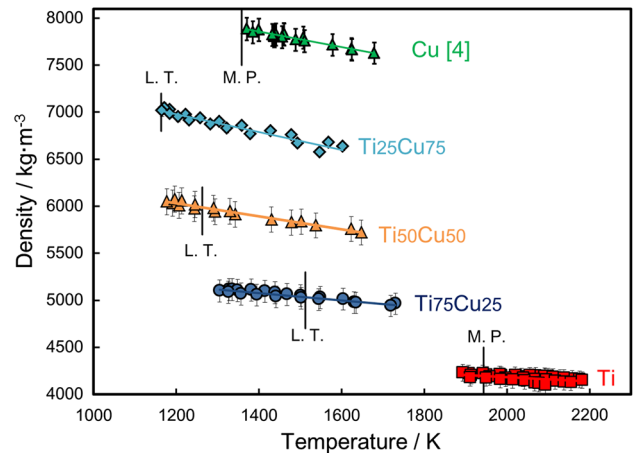


**Figure 1** Temperature dependence of density of Ti–Cu melts. Error bar shows expanded uncertainty. Black line indicates the melting point or liquidus temperature.

were 0.0751–0.0765 and 0.0597–0.0815 mass%, respectively.

From these results, we confirmed that the oxygen content did not change during the measurement.

The temperature dependence of the density of liquid Ti is shown in Fig. 1 together with alloy data, which is given by a linear function of temperature in Table 1. The present results show good agreement with previous results [7–19] within the uncertainty, except for the data obtained with the ESL method reported by Paradis et al. [20]. Ozawa et al. [15] mentioned that it is difficult to maintain a rotationally symmetrical shape of liquid Ti with respect to the vertical axis in ESL measurements.

### Ti–Cu system

The temperature dependences of the densities of the Ti–Cu melts are shown in Fig. 1. The density of pure Cu was reported in our previous work [4]. For all alloy compositions, densities are expressed as a linear function of temperature including a supercooled liquid region. The densities ( $\rho$ ) of the melts are represented by the following equation:

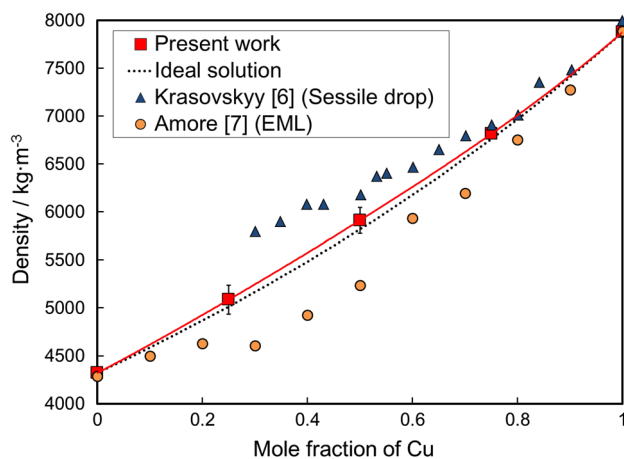
$$\rho = \rho_L + \beta(T - T_L), \quad (1)$$

where  $\rho_L$  is the density at the liquidus temperature ( $T_L$ ) of the sample and  $\beta$  is its temperature coefficient. Values of density for the Ti–Cu melts are summarized in Table 1.

The composition dependence of the density of Ti–Cu melts at 1373 K is shown in Fig. 2. The density of liquid Ti at 1373 K was estimated by linear extrapolation. For

**Table 1** Melt density as a function of temperature

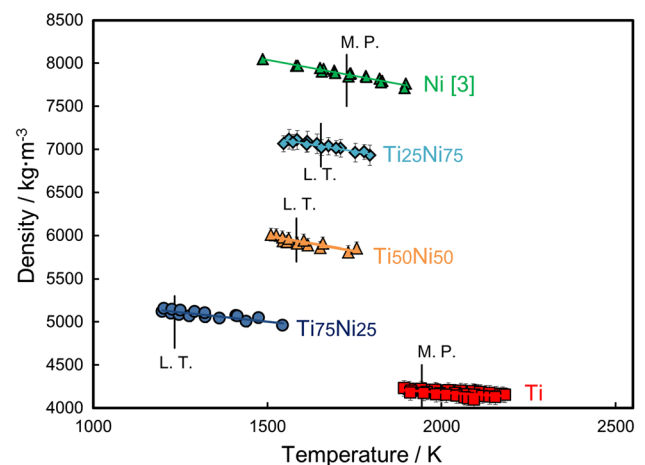
System	Temperature range (K)	Melting point or liquidus temperature, $T_L$ (K)	Density at $T_L$ , $\rho_L$ ( $\text{kg m}^{-3}$ )	Temperature coefficient, $\beta$ ( $\text{kg m}^{-3} \text{K}^{-1}$ )
Ti	1893–2182	1943	4195	– 0.220
Ti <sub>75</sub> Cu <sub>25</sub>	1305–1731	1512	5032	– 0.386
Ti <sub>50</sub> Cu <sub>50</sub>	1177–1647	1263	5989	– 0.697
Ti <sub>25</sub> Cu <sub>75</sub>	1170–1618	1163	7012	– 0.943
Cu [4]	1371–1679	1358	7890	– 0.815
Ti <sub>75</sub> Ni <sub>25</sub>	1199–1545	1234	5119	– 0.429
Ti <sub>50</sub> Ni <sub>50</sub>	1511–1757	1583	5939	– 0.693
Ti <sub>25</sub> Ni <sub>75</sub>	1547–1794	1653	7041	– 0.646
Ni [3]	1488–1898	1728	7875	– 0.740

**Figure 2** Composition dependence of the density of Ti–Cu melts at 1373 K.

comparison, literature data [6, 7] are also plotted in Fig. 2. The error bars presented in Figs. 1 and 2 present the expanded uncertainty evaluated in “Uncertainty analysis” section. A considerable discrepancy exists between the two datasets obtained previously [6, 7]. One dataset, measured with the sessile drop method by Krasovskyy and Naidich [6], showed positive deviation from the ideal solution model presented by the dotted line. The other dataset measured with the electromagnetic levitation (EML) method by Amore et al. [7] presented a negative deviation from the ideal solution model. The present results showed a small positive deviation from the ideal solution model. These differences are discussed in “Uncertainty analysis” section.

### Ti–Ni system

The temperature dependences of the densities of Ti–Ni melts are shown in Fig. 3. The density of pure Ni has been reported in our previous work [3]. For all

**Figure 3** Temperature dependence of the density of Ti–Ni melts.

alloy compositions, densities are expressed as a linear function of temperature, which includes the supercooled liquid region, as summarized in Table 1. The composition dependence of the density of the Ti–Ni melts at 1545 K is presented in Fig. 4. The density of Ti at 1545 K was estimated by linear extrapolation. The error bars in Figs. 3 and 4 show the expanded uncertainty evaluated in “Uncertainty analysis” section. The present work agrees with previous results measured using the ESL method by Zou et al. [8].

## Discussion

### Uncertainty analysis

The uncertainty of the density measurements was evaluated on the basis of the *Guide to the Expression of Uncertainty in Measurement* (GUM) [21] with the following equations:

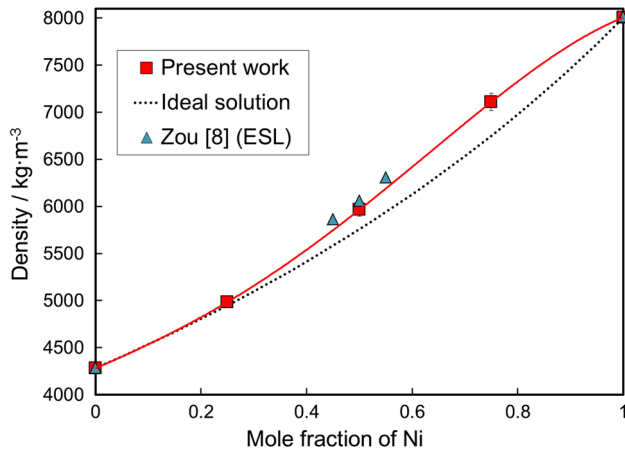


**Figure 4** Composition dependence of the density of Ti–Ni melts at 1545 K.

$$u^2(\rho) = \left(\frac{\partial \rho}{\partial V}\right)^2 u^2(V) + \left(\frac{\partial \rho}{\partial m}\right)^2 u^2(m); \tag{2}$$

$$u^2(V) = u_1^2(V) + u_2^2(V); \tag{3}$$

$$u^2(m) = u_3^2(m) + u_4^2(m), \tag{4}$$

where  $u(\rho)$  is the combined standard uncertainty in the density measurement, and  $u(V)$  and  $u(m)$  are the uncertainties of sample volume and mass, respectively. As an example, the uncertainty evaluation in the density measurement of liquid Ti at 2182 K is listed in Table 2. The parameter  $u_1(V)$  is the standard deviation in the volume obtained from analysis of 2000 images,  $u_2(V)$  is the accuracy of the conversion from pixels to real length,  $u_3(m)$  is the uncertainty in mass caused by sample evaporation, and  $u_4(m)$  is the uncertainty in mass determined from the accuracy of the balance. Table 2 shows that the main contribution to the uncertainty is  $u_1(V)$  and the expanded

uncertainty  $U = 2u(\rho)$  (95.45% confidence) is  $102 \text{ kg m}^{-3}$ , which corresponds to 2.5% of the density value ( $4150 \text{ kg m}^{-3}$ ). In this study, the expanded uncertainty for all measurements ranged from 1.2 to 2.5%.

Krasovskyy and Naidich [6] evaluated the uncertainty to be 0.5% in their density measurements of Ti–Cu melts by the sessile drop method. However, it is difficult to maintain a rotationally symmetrical shape in the sessile drop method, which might cause the actual uncertainty to be greater than that evaluated. Amore et al. [7] evaluated the uncertainty in their density measurement to be 4%. Thus, the densities measured by the EML method without a static magnetic field had a large uncertainty, which was caused by rotationally asymmetrical components of the surface oscillation such as  $l = 2, m = 2$  oscillation mode.

### Molar volume

The partial molar volume of component  $i$  ( $V_i$ ) in an  $i$ – $j$  binary system is expressed by the following equation:

$$V_i = V - x_j \left(\frac{\partial V}{\partial x_j}\right), \tag{5}$$

where  $V$  is the molar volume of the system and  $x_j$  is the mole fraction of  $j$ . Figure 5 shows the composition dependence of  $V, V_{\text{Ti}}$  and  $V_{\text{Cu}}$  for Ti–Cu melts at 1373 K. Figure 6 shows the composition dependence of  $V, V_{\text{Ti}}$  and  $V_{\text{Ni}}$  for Ti–Ni melts at 1545 K. The error bars in Figs. 5 and 6 present the expanded uncertainty. In this calculation, the densities of liquid Ti at 1373 and 1545 K were estimated by linear extrapolation. The values of  $V_{\text{Cu}}$  at undercooled region are in

**Table 2** Uncertainty evaluation in density measurement for liquid Ti at 2182 K

Cause	Standard uncertainty	Sensitivity coefficient	Contribution
Uncertainty of volume: $u(V)$	$1.12 \times 10^{-9} \text{ m}^3$	$\frac{\partial \rho}{\partial V} = -4.58 \times 10^{10} \text{ kg m}^{-6}$	$- 51.3 \text{ kg m}^{-3}$
Variation of volume: $u_1(V)$	$9.94 \times 10^{-10} \text{ m}^3$	$\frac{\partial \rho}{\partial V} = -4.58 \times 10^{10} \text{ kg m}^{-6}$	$- 45.5 \text{ kg m}^{-3}$
Accuracy of convert from pixels to real length: $u_2(V)$	$5.08 \times 10^{-10} \text{ m}^3$	$\frac{\partial \rho}{\partial V} = -4.58 \times 10^{10} \text{ kg m}^{-6}$	$23.3 \text{ kg m}^{-3}$
Accuracy of convert from pixels to real length: $u_2(r)$	$5.21 \times 10^{-6} \text{ m}$	$\frac{\partial V}{\partial r} = 9.75 \times 10^{-5} \text{ m}^2$	$u_2(V) = 5.08 \times 10^{-10} \text{ m}^3$
Uncertainty of mass: $u(m)$	$4.76 \times 10^{-8} \text{ kg}$	$\frac{\partial \rho}{\partial m} = 1.10 \times 10^7 \text{ m}^3$	$0.53 \text{ kg m}^{-3}$
Mass change of sample: $u_3(m)$	$4.75 \times 10^{-8} \text{ kg}$	$\frac{\partial \rho}{\partial m} = 1.10 \times 10^7 \text{ m}^3$	$0.52 \text{ kg m}^{-3}$
Accuracy of balance: $u_4(m)$	$\frac{5}{\sqrt{3}} \times 10^{-9} \text{ kg}$	$\frac{\partial \rho}{\partial m} = 1.10 \times 10^7 \text{ m}^3$	$0.06 \text{ kg m}^{-3}$
Combined standard uncertainty $u(m)$			$51.3 \text{ kg m}^{-3}$
Expanded uncertainty $U = 2u(m)$			$102 \text{ kg m}^{-3}$

$\rho = 4150 \text{ kg m}^{-3}$  for liquid Ti at 2182 K

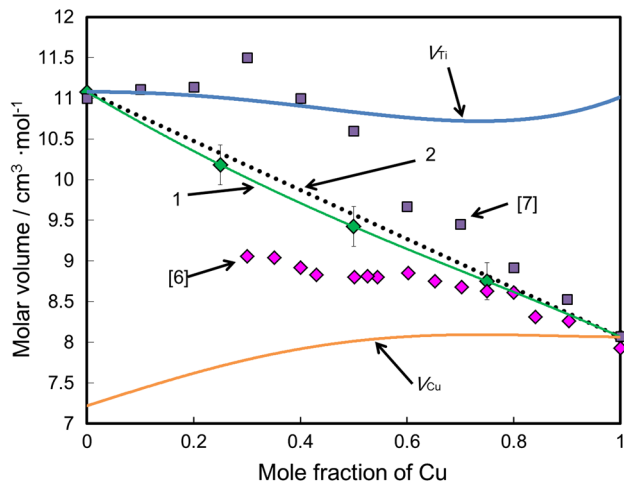


**Figure 5** Composition dependence of molar volume of Ti–Cu melts at 1373 K. 1: Present work, 2: ideal solution,  $V_{Ti}$ : partial molar volume of Ti,  $V_{Cu}$ : partial molar volume of Cu, Krasovskyy and Naidich [6] (sessile drop), Amore et al. [7] (electromagnetic levitation).

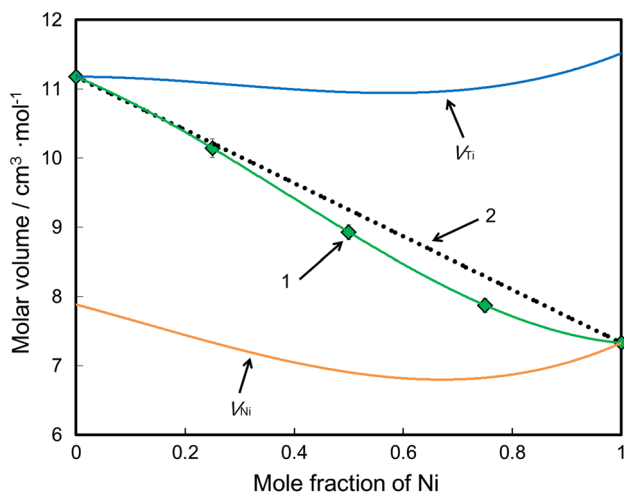


**Figure 6** Composition dependence of molar volume of Ti–Ni melts at 1545 K. 1: Present work, 2: ideal solution,  $V_{Ti}$ : partial molar volume of Ti,  $V_{Ni}$ : partial molar volume of Ni.

good agreement with reported by Kaptay; additionally, the values of  $V_{Ni}$  at whole measurement temperature region are in agreement with the reported values [22]. The values of  $V_{Cu}$  in the Ti–Cu melts remained almost constant with composition within the range  $0.5 < x_{Cu} < 1$  as shown in Fig. 5. This behavior is consistent with atomic coordination around Cu atoms, as reported by Fukunaga et al. [23, 24]. They reported that Cu–Cu atom pairs prefer to occupy the first nearest coordination site in Ti–Cu glasses studied by pulsed neutron total scattering

and X-ray diffraction techniques. Conversely, the values of  $V_{Ni}$  in the Ti–Ni melts decreased with increasing Ti content in the Ni-rich melts as shown in Fig. 6. The chemical short-range structure of the Ti–Ni glasses was different from that in the Ti–Cu glasses as reported by Fukunaga et al. [23, 24]. They reported that Ni–Ti atom pairs preferentially occupy the first nearest coordination in the Ti–Ni glasses, which is consistent with the behavior of  $V_{Ni}$  in the Ti–Ni melts.

### Excess volume

The excess volume ( $V^E$ ) of a binary melt is expressed by the following equation:

$$V^E = V - \sum_{i=1}^2 x_i \left( \frac{m_i}{\rho_i} \right), \quad (6)$$

where  $\rho_i$  and  $m_i$  are the density and molar mass of component  $i$ , respectively. The excess volume  $V^E$  is zero for an ideal solution. Figures 7 and 8 show the composition dependence of the excess volume for Ti–Cu and Ti–Ni melts determined from this study. The excess volume of Ti–Cu obtained in the present work had small negative values. Conversely, the excess volume of Ti–Cu melts reported by Amore et al. [7] showed positive values, which showed significant discrepancies with the results in the present work. These discrepancies suggest that the data reported by Amore et al. were affected by rotationally asymmetrical components of surface oscillation in the levitated

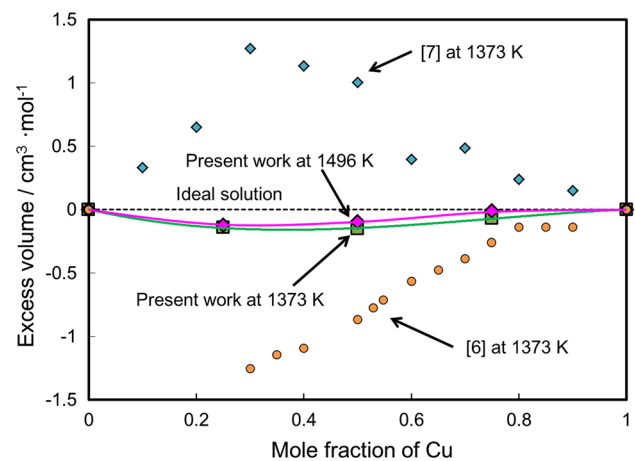


**Figure 7** Composition dependence of excess volume of Ti–Cu melts. Present work at 1373 and 1496 K, dashed line: ideal solution, Krasovskyy and Naidich [6] at 1373 K (sessile drop), Amore et al. [7] at 1373 K (electromagnetic levitation).

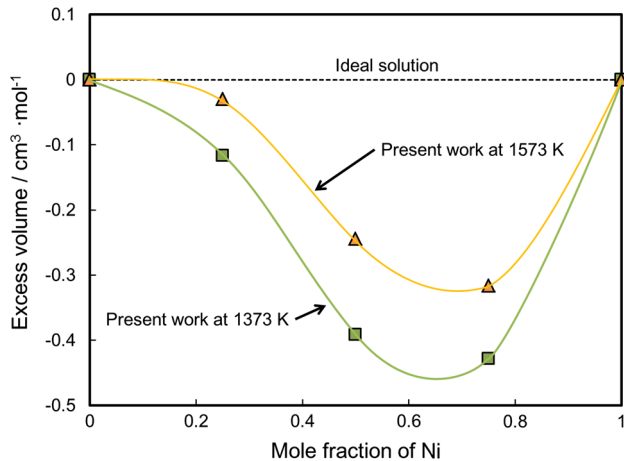


**Figure 8** Composition dependence of excess volume of Ti–Ni melts. Present work at 1373 and 1573 K; dashed line: ideal solution.

droplet. The excess volume of Ti–Ni melts presents negative values over the whole composition range, which approached the ideal solution model with increasing temperature. This temperature dependence of molar volume obeys the Lupis–Elliott rule [25, 26].

### Excess volume and thermodynamic correlations

In 1988, Iida and Guthrie [2] summarized the relationships between  $V^E$  and thermodynamic properties of binary alloy systems. According to their report, the enthalpy of mixing ( $\Delta_{\text{mix}}H$ ) or excess entropy is expected to have negative values for negative  $V^E$ , which are observed for compound-forming systems. In our previous paper [3],  $V^E$  was discussed based on both enthalpy of mixing and excess Gibbs energy ( $G^E$ ), because  $\Delta_{\text{mix}}H$  reflects only the interatomic interaction. Here, again we discuss the  $V^E$  based on both  $\Delta_{\text{mix}}H$  and  $G^E$  for the Ti–Cu and Ti–Ni systems. First, the values of  $\Delta_{\text{mix}}H$  and  $G^E$  for the Ti–Cu and Ti–Ni systems are reviewed as follows.

For the Ti–Cu melt, Yokokawa and Kleppa [27] measured  $\Delta_{\text{mix}}H$  by high-temperature reaction calorimetry at 1372 K. Turchanin and Nikolaenko [28] measured  $\Delta_{\text{mix}}H$  by calorimetry at 1873 K. Turchanin et al. [29] measured  $\Delta_{\text{mix}}H$  by solution calorimetry at 1573 and 1873 K and calculated  $G^E$  by CALPHAD. Kleppa and Watanabe [30] measured  $\Delta_{\text{mix}}H$  by high-temperature reaction calorimetry at 1373 K. The values reported by Yokokawa and Kleppa [27], Turchanin et al. [28, 29] and Kleppa and

Watanabe [30] showed different compositional dependences among the researchers. In addition, Yokokawa and Kleppa [27] and Kleppa and Watanabe [30] did not explain their experimental uncertainty. Sommer et al. [31] measured  $\Delta_{\text{mix}}H$  and  $G^E$  by the Knudsen effusion method at 1496 K.

For Ti–Ni melts, Murray [5] calculated  $\Delta_{\text{mix}}H$  based on the regular solution at an unknown temperature. Luck and Arpshofen [32] determined  $\Delta_{\text{mix}}H$  by vacuum and SETARAM calorimeter at 1741 and 1838 K. Esin et al. [33] measured  $\Delta_{\text{mix}}H$  by vacuum calorimetry at 2000 K. Thiedemann et al. [34] measured  $\Delta_{\text{mix}}H$  by EML alloying calorimetry at 1800 and 1980 K. However, Esin et al. [33] and Thiedemann et al. [34] did not measure  $\Delta_{\text{mix}}H$  around the 0.5 mole fraction. German and Pierre [35] measured  $\Delta_{\text{mix}}H$  and  $G^E$  by Knudsen cell mass spectrometry at 1873 K. Kajikawa et al. [36] calculated  $\Delta_{\text{mix}}H$  and  $G^E$  by Thermo-Calc at 1873 K, but they did not provide details of the calculation methods and their temperature range is higher than that of our density measurements. Turchanin et al. [37] measured  $\Delta_{\text{mix}}H$  by isoperibolic calorimetry at 1873 K.

On the basis of these previous studies, correlations between  $G^E$  and  $V^E$  and between  $\Delta_{\text{mix}}H$  and  $V^E$  are plotted in Fig. 9a, b, respectively, together with other binary systems at 0.5 mole fraction. Here, we used the  $\Delta_{\text{mix}}H$  and  $G^E$  values reported by Sommer et al. [31], Luck and Arpshofen [32] and German and Pierre [35] to draw Fig. 9. These values are summarized in Table 3. In this study, both the Ti–Cu and Ti–Ni systems have negative  $V^E$  with negative  $\Delta_{\text{mix}}H$ , which indicates these are both compound-forming systems [5]. As shown in Fig. 9b, the Ti–Cu system follows the correlation proposed by Iida and Guthrie [2]. However, the Ti–Ni system has a small negative  $V^E$ , although it has a large negative  $\Delta_{\text{mix}}H$ . As shown in Fig. 9, there is a stronger correlation between  $G^E$  and  $V^E$  than that between  $\Delta_{\text{mix}}H$  and  $V^E$ , which means that entropy of mixing significantly affected the correlation, especially for compound-forming systems.

### Summary

We used a combination of EML and a static magnetic field to measure the density of Ti–X (X = Cu, Ni) melts over a range of mole fractions accurately within an expanded uncertainty from 1.2 to 2.5%. The densities were measured over a wide temperature range

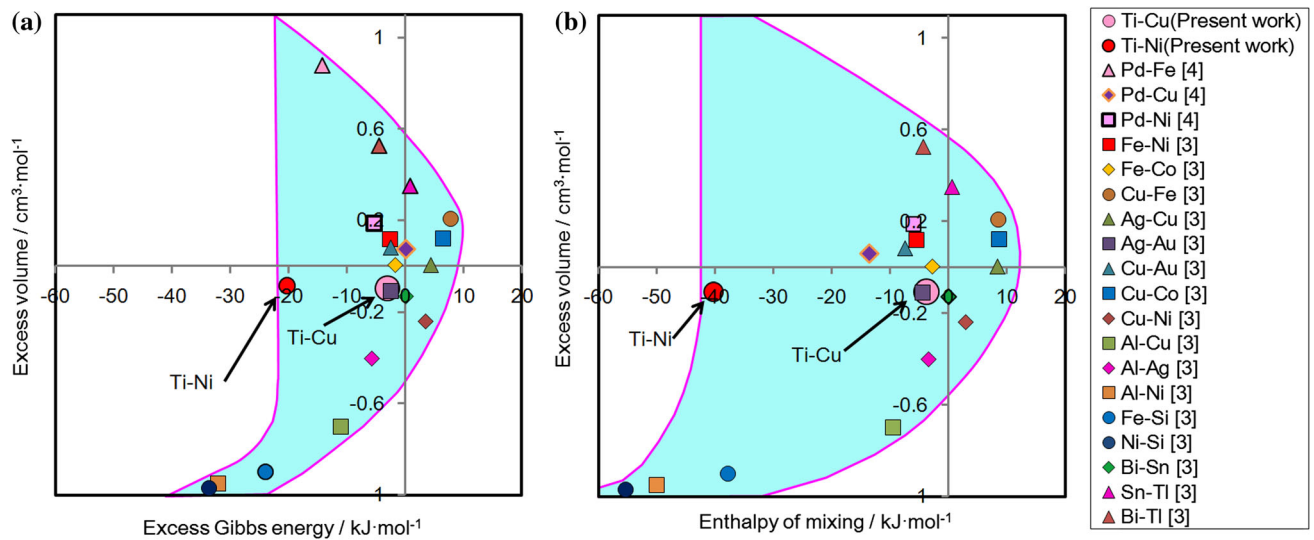


**Figure 9** **a** Correlation between excess Gibbs energy and excess volume and **b** correlation between enthalpy of mixing and excess volume for various binary melts at 0.5 mol fraction.

**Table 3** Relationship between thermodynamic properties and excess volume of binary alloys melts at 0.5 mole fraction

System	Temperature (K)	Excess volume ( $\text{cm}^3 \text{mol}^{-1}$ )	Excess Gibbs energy ( $\text{kJ mol}^{-1}$ )	Enthalpy of mixing ( $\text{kJ mol}^{-1}$ )
Ti–Cu	1496	– 0.10	– 2.98 [29]	– 3.67 [29]
Ti–Ni	1741	– 0.11	No data	– 40.17 [30]
	1773	– 0.09	– 20.18 [33]	No data

including the supercooled region. The densities varied linearly with temperature. Excess volumes of these melts were negative over the entire composition range. The Ti–Cu system has a small negative  $V^E$  with a small negative  $\Delta_{\text{mix}}H$ , which is similar to the behavior of other binary systems. However, the Ti–Ni system has a small negative  $V^E$ , despite its large negative  $\Delta_{\text{mix}}H$ . A stronger correlation can be found between  $G^E$  and  $V^E$  than that between  $\Delta_{\text{mix}}H$  and  $V^E$ .

## Acknowledgements

The authors thank Professor Jürgen Brillo (German Aerospace Center) and Associate Professor Hidekazu Kobatake (Hirosaki University) for helpful discussions and critical comments. This work was supported by Japan Society for the Promotion of Science (JSPS) KAKENHI Grant Nos. 26249113 and 18J11474.

## Compliance with ethical standards

**Conflict of interest** The authors declare that they have no conflict of interest.

## References

- [1] Scatchard G (1937) Change of volume on mixing and the equations for non-electrolyte mixtures. *Trans Faraday Soc* 33:160–166
- [2] Iida T, Guthrie RIL (1988) *The physical properties of liquid metals*. Clarendon, Oxford, pp 68–69
- [3] Watanabe M, Adachi M, Fukuyama H (2016) Densities of Fe–Ni melts and thermodynamic correlations. *J Mater Sci* 51:3303–3310. <https://doi.org/10.1007/s10853-015-9644-2>
- [4] Watanabe M, Adachi M, Fukuyama H (2018) Correlation between excess volume and thermodynamic functions of liquid Pd–X (X = Fe, Cu and Ni) binary systems. *J Chem Therm* 130:9–16
- [5] Murray JL (1987) *Phase diagram of binary titanium alloys*. ASM International, Materials Park
- [6] Krasovskyy V, Naidich Y (2004) Surface tension and specific volume of copper-titanium melts measured by the sessile drop method. *J Adhes Sci Technol* 18(4):465–471
- [7] Amore S, Delsante S, Kobatake H, Brillo J (2013) Excess volume and heat of mixing in Cu–Ti liquid mixture. *J Chem Phys.* 139:064504
- [8] Zou K, Wang HP, Yang SJ, Hu L, Wei B (2017) Anomalous temperature dependence of liquid state density for Ni50Ti50

- alloy investigated under electrostatic levitation state. *Chem Phys Lett* 681:101–104
- [9] Saito T, Shiraishi Y, Sakuma Y (1969) Density measurement of molten metals by levitation technique at temperatures between 1800 and 2200 °C. *Trans ISIJ* 9:118–126
- [10] Wessing JJ, Brillo J (2017) Density, molar volume, and surface tension of liquid Al–Ti. *Meta Mater Trans A* 48:868–882
- [11] Zhou K, Wang HP, Chang J, Wei B (2015) Experimental study of surface tension, specific heat and thermal diffusivity of liquid and solid titanium. *Chem Phys Lett* 639:105–108
- [12] Lee GW, Jeon S, Park C, Kang DH (2013) Crystal–liquid interfacial free energy and thermophysical properties of liquid Ti using electrostatic levitation: hypercooling limit, specific heat, total hemispherical emissivity, density, and interfacial free energy. *J Chem Thermodyn* 63:1–6
- [13] Paradis PF, Rhim WK (2000) Non-contact measurement of thermophysical properties of titanium at high temperature. *J Chem Thermodyn* 32:123–133
- [14] Ishikawa T, Paradis PF (2005) Thermophysical properties of molten refractory metals measured by an electrostatic levitator. *J Electron Mater* 34:1526–1532
- [15] Ozawa S, Kudo Y, Kuribayashi K, Watanabe Y, Ishikawa T (2017) Precise density measurement of liquid titanium by electrostatic levitator. *Mater Trans* 58:1664–1669
- [16] Pottlacher G (2010) High temperature thermophysical properties of 22 pure metal. Keiper, Graz
- [17] Mills KC (2002) Recommended values of thermophysical properties for selected commercial alloys. Woodhead published Ltd, Cambridge, p 205
- [18] Wang HP, Yang SJ, Wei BB (2012) Density and structure of undercooled liquid titanium. *Chin Sci Bull* 57:719–723
- [19] Gale WF, Totemeier TC (2004) *Smithells 'Metals reference book'*, 8th edn. Elsevier, Amsterdam
- [20] Paradis PF, Ishikawa T, Yoda S (2008) Experiments in metals science on the ground and in reduced gravity using electrostatic levitation. *Adv Space Res* 41:2118–2125
- [21] Evaluation of measurement data—Guide to the expression of uncertainty in measurement, (2008) JCGM 100:2008
- [22] Kaptay O (2015) Approximated equations for molar volumes of pure solid fcc metals and their liquids from zero Kelvin to above their melting points at standard pressure. *J Mater Sci* 50:678–687. <https://doi.org/10.1007/s10853-014-8627-z>
- [23] Fukunaga T, Kai K, Naka M, Watanabe N, Suzuki K (1982) High resolution short-range structure of Ni–Ti and Cu–Ti alloy glasses by Pulsed neutron total scattering. In: *Proceedings of 4th international conference on rapidly quenched metals (Sendai 1981)*, vol. 1, pp 347–350
- [24] Fukunaga T, Hayashi N, Kai K, Watanabe N, Suzuki K (1983) Chemical short-range structure of  $Ni_xTi_{1-x}$  ( $x = 0.26–0.40$ ) alloy glasses. *Physica* 120B:352–356
- [25] Lupis CHP, Elliott JF (1966) Correlation between excess entropy and enthalpy functions. *Trans. Metall. Soc. AIME* 236:130
- [26] Kaptay O (2012) On the tendency of solutions to tend toward ideal solutions at high temperatures. *Metall. Met. Trans. A* 43A:531–543
- [27] Yokokawa H, Kleppa OJ (1981) Thermochemistry of liquid alloys of transition metals II. (copper + titanium) at 1372 K. *J Chem Thermodyn* 13:703–715
- [28] Turchanin MA, Nikolaenko IV (1996) Enthalpies of solution of titanium, zirconium, and hafnium in liquid copper. *J Alloys Compd* 236:236–242
- [29] Turchanin MA, Agraval PG, Fesenko AN, Abdulov AR (2005) Thermodynamics of liquid alloys and metastable phase transformations in the copper-titanium system. *Powder Metall Met Ceram* 44:259–270
- [30] Kleppa OJ, Watanabe S (1982) Thermochemistry of alloys of transition metals: part III. Copper-silver, -titanium, -zirconium, and -hafnium at 1373 K. *Meta Mater Trans B* 13B:391–401
- [31] Sommer F, Klappert KH, Arpshofen I, Predel B (1982) Thermodynamics investigations of liquid copper-titanium alloys. *Z Metallkd* 73:581–584
- [32] Luck R, Arpshofen I (1988) Calorimetric determination of the enthalpies of formation of liquid Ni–Ti alloys. *Thermochim Acta* 131:171–181
- [33] Esin YO, Valishev MG, Ermakov AF, Gel'd PV, Petrushevskii MS (1981) The enthalpies of formation of liquid germanium-titanium and nickel–titanium alloys. *Russ J Phy Chem* 55:753–754
- [34] Thiedemann U, Rösner-Kuhn M, Drewes K, Kuppermann G, Froberg MG (1999) Temperature dependence of the mixing enthalpy of liquid Ti–Ni and Fe–Ti–Ni alloys. *J Non-Cryst Solids* 250–252:329–335
- [35] German RM, Pierre GS (1972) The high temperature thermodynamic properties of Ni–Ti alloys. *Met Trans* 3:2819–2823
- [36] Kajikawa K, Oikawa K, Takahashi F, Yamada H, Anzai H (2010) Reassessment of liquid/solid equilibrium in Ni-rich side of Ni–Nb and Ni–Ti systems. *Mater Trans* 51:781–786
- [37] Turchanin MA, Belokonenko IV, Agraval PG (2001) Heats of formation of liquid Nickel alloys with group IVA metals. *Raspilavy* 3:53–60